Ring Morphology and pH Effects in 2D and 1D $Co(OH)_2$ Liesegang Systems

Layla Badr and Rabih Sultan*

Department of Chemistry, American University of Beirut, P.O. Box 11-0236, 1107 2020 Riad El Solh, Beirut, Lebanon

Received: October 27, 2008; Revised Manuscript Received: April 16, 2009

We study the factors that affect the morphology of $Co(OH)_2$ Liesegang rings, in a way to obtain concentric rings with large spacing, upon an appropriate variation in the experimental conditions. Such well-resolved patterns are obtained under optimum conditions: decrease in the concentration of the outer electrolyte, increase in the concentration of both the inner electrolyte and the gelatin in the hosting gel medium, and increase in the strength of a constant radial electric field applied across the pattern domain. The effect of pH on the bands in a 1D $Co(OH)_2$ Liesegang pattern is also investigated. The initial pH of the diffusing solution plays a central role in altering the band morphology, because the outer electrolyte (NH_4OH) is a base, strongly affected by the H^+ equilibrium. The number of bands decreases and the interband spacing increases with decreasing pH of the NH_4OH solution. The pattern morphology in that case is controlled by the NH_4Cl/NH_4OH ratio.

1. Introduction

Periodic precipitation, or Liesegang banding,[1] has fascinated scientists for over a century and stimulated the launch of a multitude of experiments and theoretical studies.[2,3] Beautiful bands of precipitate in a tube (1D) or concentric rings in a Petri dish (2D) form as an electrolyte diffuses into a gel medium embedding one of its coprecipitate ions. The $Co(OH)_2$ Liesegang system[4,5] (from Co^{2+} and NH_4OH) has interesting dynamical properties, essentially emerging from the redissolution of the upper $Co(OH)_2$ bands[6] due to complexation of Co^{2+} with the ammonia ligand. The chemical reactions involved are as follows.

Precipitation:

$$Co^{2+}(aq) + 2NH_4OH(aq) \rightarrow Co(OH)_2(s) + 2NH_4^+(aq) \quad (1)$$

Redissolution:

$$Co(OH)_2(s) + 6NH_4^+(aq) \rightarrow Co(NH_3)_6^{2+}(aq) + 2H_2O(l) + 4H^+(aq) \quad (2)$$

In 2D, the concentric rings at the center of the pattern disappear in a synchronized manner with the precipitate ring formation toward the periphery.[7] Similar Liesegang systems with redissolution feature the HgI_2/HgI_4^{2-}[8] and the $Cr(OH)_3/Cr(OH)_4^-$[9] systems. A theoretical model for simulating the $Co(OH)_2$ Liesegang system, based on the model of Müller and Polezhaev,[10] was set forth by Al-Ghoul and Sultan.[11] It incorporates supersaturation, nucleation, kinetics of particle growth coupled to diffusion, as well as dissolution due to complex formation. The calculations were found to agree qualitatively with the experimental results.

The morphology of Liesegang patterns can, to a great extent, be controlled by a proper choice of the experimental parameters.[7] It was established that four major routes can be followed to obtain a well-resolved pattern with increased band spacing: (1) decreasing the concentration of the diffusing outer electrolyte;[12] (2) increasing the concentration of the gel material;[13] (3) applying an electric field in the direction of the propagation;[14−17] and (4) increasing the concentration of the electrolyte in the gel (inner electrolyte).[4]

In other words, any factor that would slow down the diffusive flux (factors 1 and 2) or hinder the precipitate formation by delaying the buildup of the concentration product $[Co^{2+}][OH^-]^2$ (factors 3 and 4) would result in an increase in the band spacing.

The morphology of the precipitate pattern is also influenced by a variation in temperature. At high temperatures, fewer bands are formed with increased distances between them.[18] The presence of two[19,20] or three[21] competitor coprecipitate ions can dramatically alter the dynamics of pattern formation, sometimes increasing the level of rhythmicity in a complex manner.[21] The morphology of the pattern will reflect the competition in precipitation (and redissolution in specific systems) with a common diffusing electrolyte.

Interest in steering the fabrication of Liesegang patterns spans macroscopic,[7] mesoscopic,[22] microscopic,[23] and nanostructure[24] systems. Using the so-called wet stamping technique (WETS),[23] regular arrays and bas-reliefs of microscopic precipitate structures of arbitrary shapes were generated by placing droplets on a wet gel or agarose stamps onto the surface of a thin film of dry gel. At the macroscopic level, Shreif et al.[7] carried out a systematic study on $Co(OH)_2$ based on a control of the first three parameters listed above, in an attempt to produce a neat and well-resolved 2D pattern of concentric rings. The appearance of the pattern was significantly transformed from a "crude", narrow-spaced pattern (Figure 1a) into a distinct pattern of rings with wide spacings (Figure 1c).

We further note that, whereas the pattern in Figure 1a is quite remote from the central source tube, the onset of bands is brought much closer to the junction after proper treatment as shown in Figure 1b and 1c. Because of a significantly lower NH_4OH concentration, redissolution via reaction 2 is tremendously suppressed. In the present study, we pursue the alteration and taming of the pattern morphology by tackling the fourth parameter. In addition to the above listed factors, we investigate the effect of varying the pH of the diffusing ammonia solution on the pattern morphological features. We shall demonstrate

* Corresponding author. E-mail: rsultan@aub.edu.lb.

10.1021/jp8094984 CCC: $40.75
Published on Web 05/21/2009

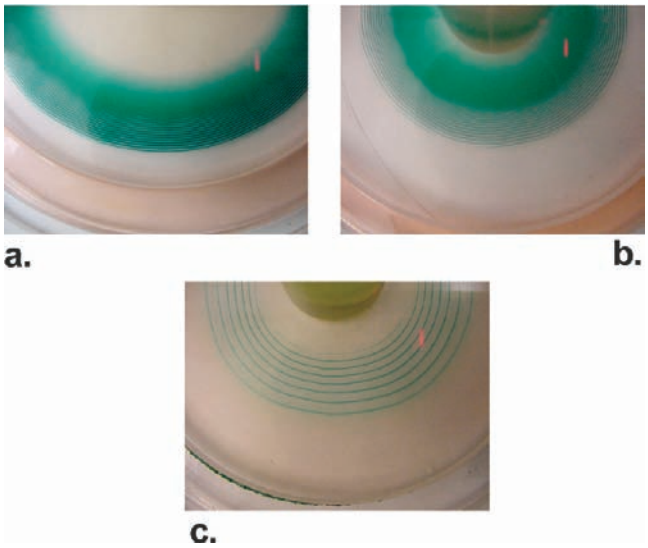

Figure 1. Motivation for this study. The change in the conditions of the experiment can significantly alter the morphological features of 2D Liesegang patterns. In all experiments, $[Co^{2+}]_0 = 0.100$ *m*. (a) 5% gelatin, $[NH_4OH]_0 = 13.3$ M, field free. (b) 7% gelatin, $[NH_4OH]_0 = 2.67$ M, field free. (c) 9% gelatin, $[NH_4OH]_0 = 1.33$ M, $V = 4.0$ V. While the decrease in $[NH_4OH]_0$ brings the pattern closer to the interface (b), it does not clear the uniform precipitate region. In frame c, the presence of an electric field and the further decrease in $[NH_4OH]_0$ clears the haze, and increases the spacing, producing the most well-resolved pattern obtained, "so far".

that such pH modification plays a central role in disturbing the balance between reactions 1 and 2, and hence paves the way toward a novel effective method for steering the dynamical and textural properties of the pattern.

2. Morphology of $Co(OH)_2$ Rings

The evolution of the $Co(OH)_2$ Liesegang pattern in two-dimensional radially symmetric gel media is studied in this section. The initial Co^{2+} electrolyte concentration is varied, and the resulting morphological characteristics are investigated, while some features related to the underlying dynamics are explored. The experiments are performed in a domain of large initial concentration difference between the electrolytes hosting the reacting ions.

The starting point is the pattern in Figure 1c, achieved after a concerted optimization of the first three conditions listed in secttion 1. It was reported[7] under the following set of conditions: $[NH_4OH]_0 = 1.33$ M, potential difference $V = 4.0$ V, and 9% gelatin, for an initial molality of $CoCl_2$ of 0.100 *m*. (The symbol *m* denotes here molal unit, mol (salt)/kg of H_2O. Note that we retain the notation $[Co^{2+}]$ for molal concentration, but the distinction from molar concentration appears by specifying the unit.) We now increase the cobalt ion concentration. The ring spacing is known to increase with increasing inner electrolyte (Co^{2+}) concentration,[4] and hence we expect to obtain more clear and distinct patterns. Four new $[CoCl_2]_0$ concentrations are inquired: 0.200, 0.300, 0.400, and 0.500 *m*, respectively. It is to be noted that those experiments are extremely sensitive to the ambient conditions and thus require a very careful control of the imposed parameters.

Experimental Section. 25.00 mL of double-distilled water was delivered by means of a volumetric pipet into a small beaker. To this volume we added the following: the required mass of $CoCl_2 \cdot 6H_2O$ (Fluka, MW 237.93, ≥98.0%), weighed to the nearest 0.1 mg, and a fixed mass of gelatin (Difco, 2.50 g).

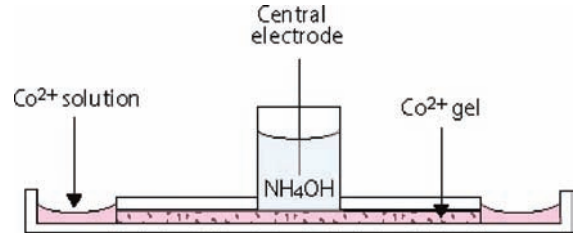

Figure 2. Diametric cross-section of the special Petri dish designed for the experiment. The gel is sandwiched between two methacrylate glass plates. The central tube contains the diffusing ammonia solution, in which a vertical electrode wire is immersed. The peripheral cavity contains the same electrolyte as in the gel (also with the same $[Co^{2+}]_0$).

This yields 8.2−8.9% gelatin (depending on the mass of $CoCl_2 \cdot 6H_2O$ used). The mixture is heated with constant stirring for a few minutes until a clear and homogeneous solution is obtained. The resulting solution is then immediately poured into a Petri dish designed especially for this type of experiment, illustrated in Figure 2.

The liquid gel, delivered through the vertical tube, spreads smoothly and evenly into the thin layer space between the two plates, without formation of air bubbles. The solution is then left to gel overnight at room temperature. On the next day, the gel is neatly cut and removed from the bottom of the cylindrical pouring tube, as well as from the peripheral cavity (see Figure 2). A tungsten wire (Aldrich, 356972-18.9G) of 0.5 mm diameter modeled into a circular ring shape is placed in the peripheral cavity of the Petri dish. Next, this cavity is filled with a $CoCl_2$ solution (of the same concentration as the gel solution), in a way to completely immerse the circular electrode. A straight tungsten wire electrode is placed vertically in the cylindrical tube. The outer (circular) electrode is connected to the negative pole of a power supply (EZ Digital Co., Ltd. GP-4303D), and the inner (straight) electrode is connected to the positive pole. A DC current under a potential difference of 4.0 V from the power generator is applied across the reaction medium. The central tube is filled with 5 mL of 1.33 M NH_4OH, and the whole setup is then placed in an air thermostat chamber maintained at $T = 20.0 \pm 0.5$ °C.

Immediately after the addition of ammonia, the field is turned on, and a homogeneous blue $Co(OH)_2$ precipitate forms at the interface between the gel and the ammonia solution, marking the instantaneous beginning of precipitation.

Results. A few hours after the addition of ammonia ($t = 0$), concentric precipitate rings start to appear. The number of rings increases as more ammonia solution diffuses into the gel. The spacing between consecutive rings increases with increasing distance from the interface between the two electrolytes, in conformity with the well-known spacing law.[25,26] Unlike most 2D Liesegang experiments in other salt systems wherein many ring distortions and defects were reported and studied,[27−29] the $Co(OH)_2$ patterns obtained here display very distinct rings of almost perfect symmetry and circular shape.

Figure 3 shows the obtained patterns of concentric circular rings, at the five different Co^{2+} concentrations. We define a number of parameters that are typically used in the characterization of the morphological features of Liesegang patterns.[26]

The average spacing ratio ρ_n between two successive rings numbered n and $n + 1$ is as follows:

$$\rho_n = \frac{x_{n+1}}{x_n} \tag{3}$$

where x_n and x_{n+1} are the locations (distances) of rings n and $n + 1$, respectively, from the junction.

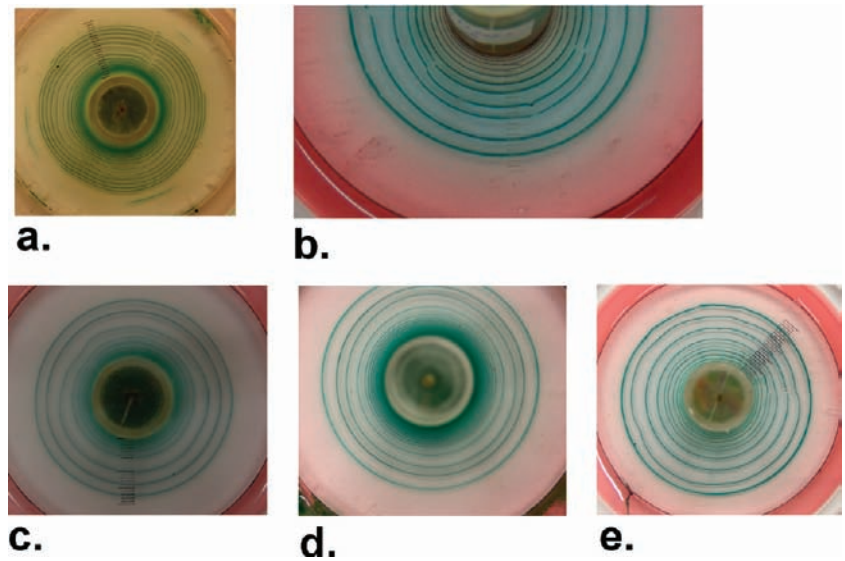

Figure 3. Results of the refined new experiments wherein $[Co^{2+}]_0$ was varied. $[NH_4OH]_0$ was decreased to 1.33 M. Gelatin concentration 9%. Inner electrolyte molal concentrations $[Co^{2+}]_0$ = (a) 0.100 *m*; (b) 0.200 *m*; (c) 0.300 *m*; (d) 0.400 *m*; and (e) 0.500 *m*. Radial electric field of potential difference $V = 4.0$ V.

TABLE 1: Spacings Δx and Average Spacing Ratio ρ for the Patterns Shown in Figure 3

$[Co^{2+}]_0$ (*m*)	ρ	Δx at distance 0.5 cm	Δx between the last two rings
0.100	1.22	0.09	0.15
0.200	1.36	0.15	0.28
0.300	1.38	0.20	0.33
0.400	1.42	0.22	0.52
0.500	1.56	0.27	0.55

The spacing between two consecutive rings from the interface is as follows:

$$\Delta x_n = x_{n+1} - x_n \tag{4}$$

In Table 1, we report the values of ρ and Δx at the five aforementioned concentrations. The latter spacing (Δx) is measured both at 0.5 cm from the junction, as well as between the last two rings formed at an average time of 26 h.

The variation of the above morphological parameters with concentration of inner electrolyte, $[Co^{2+}]_0$, is plotted in Figure 4. Clearly, both the spacing Δx and the spacing ratio ρ increase with increasing Co^{2+} concentration.

At higher cobalt ion concentration, the formation of a band consumes a larger amount of NH_4OH. The depletion in the diffusing electrolyte has a more pronounced effect than at a lower Co^{2+} concentration. The replenishment in NH_4OH consumes more time for supersaturation to be attained ($\sigma \equiv [Co^{2+}][OH^-]^2 > \sigma_{critical}$), causing the next band of $Co(OH)_2$ to form at a relatively larger spacing. This effect is tremendously enhanced by the presence of the radial electric field, wherein the charge distortion results in a more pronounced change in the gradient.[30] Note that in the absence of a field, $[Co^{2+}]$ is spatially uniform, and the gradient $\vec{\nabla}[Co^{2+}] = 0$. When the field is on, Co^{2+} is dragged toward the cathode, which results in a slower buildup of σ. Thus, at high Co^{2+} initial concentration, and in the presence of a positive field, the requirement for precipitation is doubly hindered, and a significant increase in spacing is obtained. A larger band spacing and spacing ratio are achieved by controlling both factors. By influencing the front propagation this way, we hope to be able to "architect" any desired morphology of the $Co(OH)_2$ rings pattern.

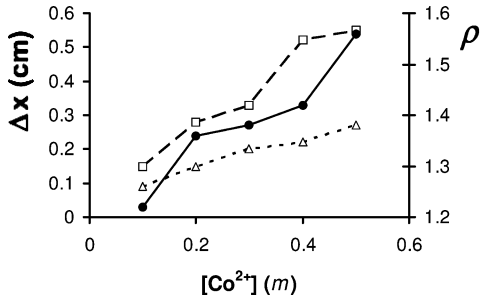

Figure 4. Variation of the spacing (Δx, left axis) and the spacing ratio (ρ, right axis) with initial Co^{2+} molal concentration ($[Co^{2+}]_0$). Small dashes with Δ, spacing at an average distance of 0.5 cm from the interface; big dashes with □, spacing between the last two rings; solid line with ●, spacing ratio.

A fifth parameter that could as well be monitored is the thickness[31] of the gel layer, which can also alter the morphology of the precipitate pattern. Whereas the effect of gel concentration was studied by Shreif et al.,[7] the gel thickness factor was not tackled. Here, both gel concentration and thickness were maintained constant throughout all of the experiments. So we would expect an even higher ability to tame the pattern by modifying and adjusting those interesting gel characteristics.

3. Effect of the pH of the Outer Electrolyte on the Band Formation in 1D

In this section, the effect of altering the pH of the outer ammonia solution (before administration into the tube) on the morphology of the $Co(OH)_2$ precipitate pattern (the Liesegang system) is studied. The study is carried out in 1D. The initial Co^{2+} inner electrolyte concentration is held constant. The pH of the outer solution experiences a spatiotemporal variation with diffusion. We use here the initial pH as the control parameter. The morphology of the pattern (number of bands, and spacing between the last two bands at a specific chosen time) is analyzed and correlated with the effect of pH.

Decreasing the pH of the diffusing ammonia solution by adding H^+ ions will interfere in the precipitation−redissolution scenario of a typical $Co(OH)_2$ Liesegang system. Initially, a concentrated ammonia solution has equal concentrations of

TABLE 2: Number of Bands and Spacing as a Function of pH

	tube no.					
	1	2	3	4	5	6
pH	13.51	12.23	11.79	11.47	10.90	10.52
no. of bands day 1	30	27	24	20	13	4
no. of bands day 3	29	26	22	17	10	3
spacing between the last two bands day 15 (cm)	0.25	0.27	0.28	0.32	0.50	0.81

ammonium and hydroxide ions, illustrated by the one-to-one stoichiometry of the equilibrium reaction:

$$NH_4OH \rightleftharpoons NH_4^+ + OH^- \quad (5)$$

Upon the addition of hydrochloric acid (HCl), the following reaction predominantly occurs:

$$NH_4OH + HCl \rightarrow H_2O + NH_4^+ + Cl^- \quad (6)$$

Hence, the hydroxide ions from ammonia will be partially neutralized by H^+ from HCl, resulting in a solution with NH_4^+ concentration dominant over OH^-. In such a situation, the precipitation of $Co(OH)_2$ will be suppressed, and the dissolution driving the formation $Co(NH_3)_6^{2+}$ will be enhanced by excess NH_4^+. We anticipate that the decrease in the pH of the ammonia solution achieved this way can significantly alter the morphology of the Liesegang pattern.

We prepare a set of NH_4OH solutions with different initial pH values, by adding HCl. The more HCl is added, the more NH_4^+ is dominant over the OH^- coprecipitate ion, and the more redissolution (reaction 2) is dominant over precipitation (reaction 1). Hence, by controlling the pH of the diffusing solution, we set forth a new method for altering and steering the morphological features of the pattern.

Experimental Section. We prepare a 0.336 *m* Co^{2+} in 6% gelatin solution as described in section 2. The mixture was heated with constant stirring until the solution started to boil. The resulting gel was then poured while hot into thin glass tubes (35 × 0.4 cm) sealed from one end. The gel was allowed to occupy two-thirds of each glass tube, and the upper level of the gel in every tube was marked to indicate the interface between the solutions of the coprecipitate ions. The tubes were allowed to stand overnight at 20.0 °C. The outer electrolyte solutions were prepared from NH_4OH stock solution (15.3 M) and concentrated HCl (12 M) as follows. A calibrated pH electrode (Orion) was dipped in a beaker containing prepipetted 25.00 mL of the stock ammonia solution. Next, concentrated HCl was added dropwise on top of the ammonia solution with continuous stirring, until the digital pH meter reads the desired pH (see the values in Table 2). Note that for tube 1, no HCl was added (i.e., the diffusing solution contains only concentrated NH_4OH). Each resulting NH_4OH solution was delivered on top of a solidified cobalt chloride gel of fixed concentration $[Co^{2+}]_0 = 0.336$ *m*. The tubes were labeled, covered with parafilm paper, and allowed to stand. Pictures of the tubes and measurements were taken and are reported here on the first, third, and fifteenth day.

Results and Discussion. In each tube with a characteristic initial pH of NH_4OH, we monitor: (I) the total number of precipitate bands (N) on days 1 and 3, and (II) the interband spacing (Δx) between the last two precipitate bands (notably on day 15). All of the measurements are recorded in Table 2.

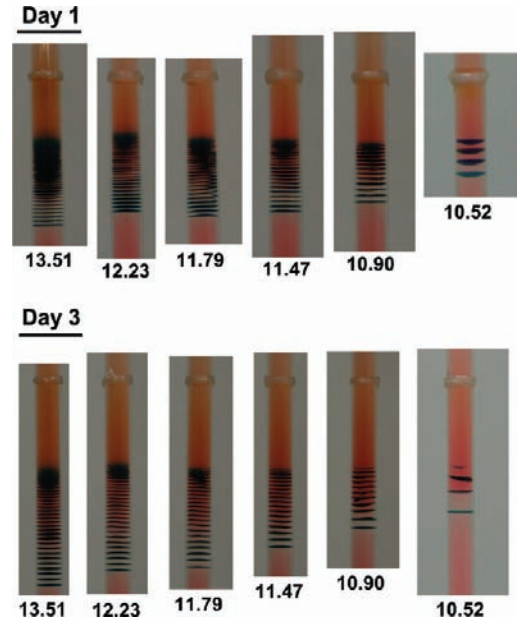

Figure 5. Obtained Liesegang patterns at different pH's of the diffusing electrolyte NH_4OH, at days 1 and 3. The pH value is marked under each tube.

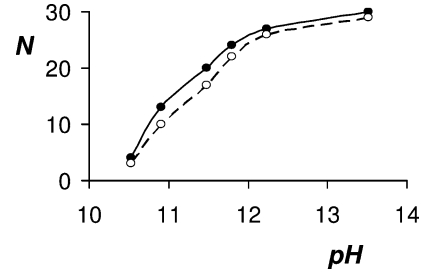

Figure 6. Variation of the number of bands at days 1 and 3 with pH. $[Co^{2+}]_0 = 0.336$ *m*. Solid line with ●, day 1; dashed line with ○, day 3.

It is clear from the pictures taken on the first and third day (displayed in Figure 5, days 1 and 3, respectively, and plotted in Figure 6) that the number of $Co(OH)_2$ bands decreases in going to lower pH. There is also a significant increase in the band spacing as time advances, at a given pH. The uniform region at the top of the pattern is gradually eliminated as we go to lower pH, as compared to the case where a concentrated ammonia solution is used (tube 1). This zone (or plug) normally results from the coalescence of a certain number of very closely spaced bands.[22] The distance from the top of the pattern to the interface at different pH's remains nearly constant. The higher NH_4^+ concentration achieved at lower pH (at the expense of NH_4OH as discussed earlier) renders the redissolution of the $Co(OH)_2$ precipitate occurring at the tail (top) of the pattern relatively much more effective. At the same time, it is very clear and distinct that precipitation (reaction 1) is tremendously suppressed due to reaction 6, which forms NH_4^+ and neutralizes OH^-. This is mostly revealed by the decrease in the number of bands N with decreasing pH, due to the shortage in OH^- (see Figure 6 and Table 2).

The last tube (pH = 10.52) shows a crucial regularization relative to the preceding one (pH = 10.9), illustrated by the clear and distinct bands and the notably increased band spacing.

This sudden pronounced decrease in N is obviously a consequence of the dominance of redissolution (2) over precipitation (1). It is also consistent with the trend observed

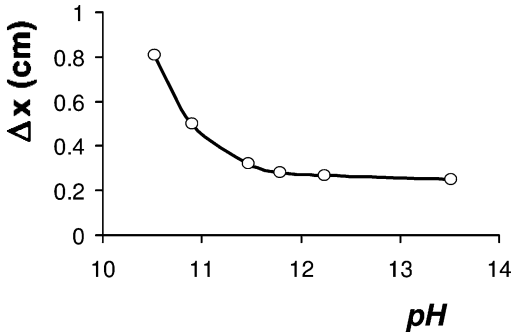

Figure 7. Variation of the spacing Δx with pH at day 15. $[Co^{2+}]_0 = 0.336$ *m*. The increase in spacing with decreasing pH starts smoothly, then suddenly goes abruptly.

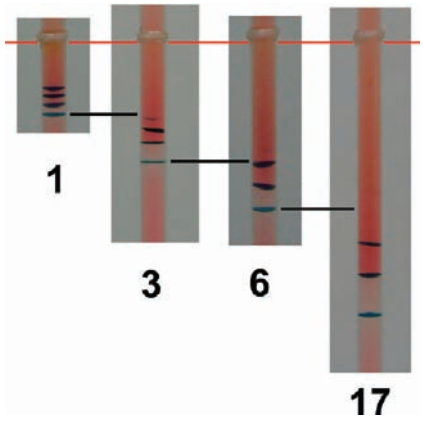

Figure 8. Time sequence of the pattern evolution at pH 10.52. Time (in days) is indicated under each tube picture. The red line marks the NH_4OH gel junction. The band spacing becomes distinctly large as time advances. The upper bands dissolve away. The black line indicates the same band at different times. Some have disappeared by dissolution.

in experiments starting with lower concentrations of the NH_4OH solution, wherein fewer and more resolved bands are observed.[7,12] The most interesting variant in the present case (as opposed to the latter experiments performed without addition of HCl, although with low $[NH_4OH]_0$) is that dissolution and precipitation are widely differentiated. This leads to the design of a pattern with a few number of bands (as few and as widely spaced as desired) in the middle of the gel region (see the last frame in Figure 5a and b).

We now focus on the second characteristic altered by varying the initial pH, the spacing between the bands (represented here by measuring the distance between the last two $Co(OH)_2$ precipitate bands). The pH variation of the spacing between the last two bands on day 15 appears in the last line of Table 2 and is plotted in Figure 7. The spacing is notably larger at lower pH. At lower OH^- concentrations from NH_4OH (lower pH), the requirement for band formation by precipitation ($\sigma = [Co^{2+}][OH^-]^2 > \sigma_{critical}$) is fulfilled with slower concentration buildup and would cause a band to form further away in space from the preceding one. Day 15 (when the effect is mostly marked) was chosen for reporting the values, because the spacing increases as time advances. The spacing between the last two precipitate bands (formed last in space and time) was found to be a representative measure here. The time evolution of the pattern at pH 10.52 is illustrated in Figure 8. The bands are notably farther away from the junction (because of marked redissolution of the top bands) and are notably well resolved by virtue of the increase in spacing as we advance in time and space. Antal et al.[22] developed a model of driven precipitation

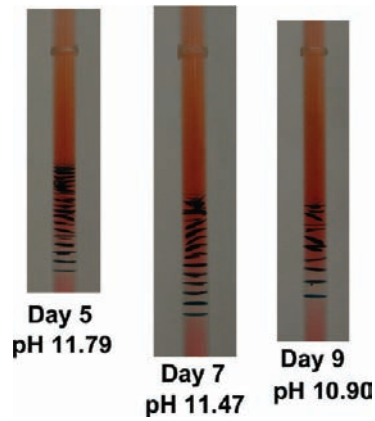

Figure 9. Band distortions start appearing at later times in the presence of acid (lower pH). This is attributed to the loosening of the gelatin gel caused by an increase in $[NH_4^+]$.

wherein phase separation is governed by a guiding field such as temperature or pH. They demonstrated that the interband spacing is controlled by the velocity of the phase separation instability front. In congruence with those findings, the pattern wavelength in the present study is determined by the pH field.

Note that distortions (nonhorizontality and partial breakage; see Figure 9) in the $Co(OH)_2$ precipitate bands were noticed at the top of the pattern. This occurs because NH_4Cl (NH_4^+ increased by adding acid) has an apparent effect in tremendously loosening the gel rigidity. Such distortions were not observed for tube 1 because no acid was added to the ammonia solution. The effect of NH_4^+ on the gel was verified by separate tests on the gel texture performed with a 2.0 M NH_4Cl solution.

This study of different $Co(OH)_2$ Liesegang systems deserves to be pursued with a systematic variation of the pH of the ammonia solution. An effective way of taming the deformation of the bands should be developed, by essentially preserving the hard texture of the gel matrix. A quantitative criterion relating $[NH_4OH]_0$, initial pH, band spacing, and number of bands is under current investigation. Such refinements constitute the subject of a forthcoming paper.

4. Conclusions

Designing and controlling patterns emerging from nonlinear reaction-diffusion dynamical systems still triggers interest and stimulates research. The fabrication of precipitate patterns and their modulation through the control of reaction and diffusion can be upgraded to develop programmed reactions, spanning parallel reaction schemes, multitasking, and the creation of multicolor and gradient patterns.[24] The crossover between regular, equidistant, and revert spacing in Liesegang structures was programmed[22] through a phase separation mechanism in a space- and time-dependent guiding field. The characteristics of the pattern (such as its wavelength) were numerically found to be directly related to the velocity of the moving front. Predesigned Liesegang patterns with prescribed wavelengths, and complex patterns with multiple-band structures, were conjectured and verified experimentally through electric current-mediated protocols.[32]

In this study, we feel we have arrived at a systematic way of controlling a host of morphological features in the $Co(OH)_2$ patterning properties, by making the appropriate changes in the experimental conditions. The study enables us to steer the pattern toward any desired set of predesigned morphological characteristics. Bands as few as only one can be attained by this technique.

Acknowledgment. This work was supported by a grant of the University Research Board (URB) at the American University of Beirut (AUB).

References and Notes

(1) Liesegang, R. E. *Chemische Fernwirkung. Lieseg. Photograph. Arch.* **1896**, *37*, 305; continued in *37*, 331.
(2) Stern, K. H. *Chem. Rev.* **1954**, *54*, 79.
(3) Henisch, H. *Crystals in Gels and Liesegang Rings*; Cambridge University Press: Cambridge, UK, 1988.
(4) Sultan, R.; Sadek, S. *J. Phys. Chem.* **1996**, *100*, 16912.
(5) Sultan, R. *Phys. Chem. Chem. Phys.* **2002**, *4*, 1253.
(6) Nasreddine, V.; Sultan, R. *J. Phys. Chem. A* **1999**, *103*, 2934.
(7) Shreif, Z.; Mandalian, L.; Abi-Haydar, A.; Sultan, R. *Phys. Chem. Chem. Phys.* **2004**, *6*, 3461.
(8) Das, I.; Pushkarna, A.; Agrawal, N. R. *J. Phys. Chem.* **1989**, *93*, 7269.
(9) Zrĭnyi, M.; Gálfi, L.; Smidróczki, É.; Rácz, Z.; Horkay, F. *J. Phys. Chem.* **1991**, *95*, 1618.
(10) Polezhaev, A. A.; Müller, S. C. *Chaos* **1994**, *4*, 631.
(11) Al-Ghoul, M.; Sultan, R. *J. Phys. Chem. A* **2001**, *105*, 8053.
(12) Chopard, B.; Droz, M.; Magnin, J.; Rácz, Z.; Zrinyi, M. *J. Phys. Chem. A* **1999**, *103*, 1432.
(13) Liesegang, R. E. *Z. Phys. Chem.* **1914**, *88*, 1.
(14) Sultan, R.; Halabieh, R. *Chem. Phys. Lett.* **2000**, *332*, 331.
(15) Lagzi, I. *Phys. Chem. Chem. Phys.* **2002**, *4*, 1268.
(16) Das, I.; Pushkarna, A.; Bhattacharjee, A. *J. Phys. Chem.* **1990**, *94*, 8968.
(17) Das, I.; Pushkarna, A.; Bhattacharjee, A. *J. Phys. Chem.* **1991**, *95*, 3866.
(18) Isemura, T. *Bull. Chem. Soc. Jpn.* **1939**, *14*, 179.
(19) Sultan, R.; Al-Kassem, N.; Sultan, A.; Salem, N. *Phys. Chem. Chem. Phys.* **2000**, *2*, 3155.
(20) Msharrafieh, M.; Al-Ghoul, M.; Batlouni, H.; Sultan, R. *J. Phys. Chem. A* **2007**, *111*, 6967.
(21) Msharrafieh, M.; Sultan, R. *ChemPhysChem* **2005**, *6*, 2647.
(22) Antal, T.; Bena, I.; Droz, M.; Martens, K.; Rácz, Z. *Phys. Rev. E* **2007**, *76*, 046203.
(23) Bensenmann, I. T.; Fialkowski, M.; Grzybowski, B. A. *J. Phys. Chem. B* **2005**, *109*, 2774.
(24) Grzybowski, B. A.; Campbell, C. J. *Mater. Today* **2007**, *10*, 38.
(25) Jablczynski, C. K. *Bull. Soc. Chim. Fr.* **1923**, *11*, 1592.
(26) Antal, T.; Droz, M.; Magnin, J.; Rácz, Z.; Zrinyi, M. *J. Chem. Phys.* **1998**, *109*, 9479.
(27) Müller, S. C.; Kai, S.; Ross, J. *Science* **1982**, *216*, 635.
(28) Krug, H.-J.; Brandtstadter, H. *J. Phys. Chem. A* **1999**, *103*, 7811.
(29) Lagzi, I.; Volford, A.; Büki, A. *Chem. Phys. Lett.* **2004**, *396*, 97.
(30) Bard, A. J.; Faulkner, L. R. *Electrochemical Methods: Fundamentals and Applications*, 2nd ed.; Wiley: New York, 1980.
(31) Toramaru, A.; Harada, T.; Okamura, T. *Physica D* **2003**, *183*, 133.
(32) Bena, I.; Droz, M.; Lagzi, I.; Martens, K.; Rácz, Z.; Volford, A. *Phys. Rev. Lett.* **2008**, *101*, 075701.

JP8094984